



Numerical Study on Propagation of Ice Breaking Shock Waves in Process of Breaking Ice by Double-Layer Charge Blasting

Xuemei Zhang^{1*}, Yuanli Wu¹, Zhigang Xie², Chaosong Kong¹ and Zhizong Tian²

¹Wuhan Leishen Special Equipment Company Ltd, China.
²Yellow River institute of Hydraulic Research, YRCC, China.

Authors' contributions

This work was carried out in collaboration among all authors. All authors read and approved the final manuscript.

Article Information

DOI: 10.9734/JERR/2021/v20i1217422

Editor(s):

(1) Dr. Djordje Cica, University of Banja Luka, Bosnia and Herzegovina.

Reviewers:

(1) Saeed Ahmed Asiri, King Abdulaziz University, Saudi Arabia.

(2) Zhenjiao Sun, Shandong University of Science and Technology, China.

Complete Peer review History: <https://www.sdiarticle4.com/review-history/73619>

Original Research Article

Received 23 June 2021
Accepted 02 September 2021
Published 03 September 2021

ABSTRACT

The ice-breaking process of the double-layer charge at a depth of 150 cm underwater is simulated by LS-DYNA. This paper analyzes the load type, shock wave pressure characteristics and propagation behavior of the double-layer charge during underwater explosion. By analyzing the impact of the shock wave pressure in the water under different charge intervals and time intervals on the shock wave pressure of the double charge, it is concluded that the peak pressure of the double charge explosion shock wave is jointly determined by the double charge. In this range, the second peak pressure value of the drug is greater than the pressure value of the first peak of the drug, and the attenuation is slow; the delay time of the upper charge has little effect on the peak pressure value of the shock wave in the water; the delay time is higher than that of the lower charge Initiation, at the same position, the total pressure peak of the shock wave formed by the delay of the upper charge is larger.

Keywords: Underwater blasting; double-layer charge; water pressure; numerical simulation.

1. INTRODUCTION

Ice cube is a common natural phenomenon in rivers in cold regions. It often directly affects the construction and use of water conservancy projects, and even triggers floods, causing serious losses to the national economy and people's livelihood. The hazards of ice are mainly manifested in ice plugs and ice dams caused by ice silt and river siltation. This will cause the upstream water level to rise sharply and cause a major risk in the floodplain [1]. Therefore, it is necessary to take measures to prevent ice jams and ice dams in the course of the river course. Among many methods to break ice plugs and ice dams, the blasting method is widely used because of its high efficiency [2]. Compared with cannon coverage and aircraft bombing, ice burst has the advantages of precise control, less secondary hazards, and high mobility. It is more and more widely used in snow prevention and disaster reduction, and has important research significance. At present, many countries in the world have achieved fruitful results in the theoretical research and application of ice and underwater blasting deicing. Mailer of the US Army Corps of Engineers used regression analysis to develop explosives based on years of underwater blasting test data, ice thickness and ice cave radius [3,4]. Liang Xiangqian studied the changes in vibration velocity and underwater shock wave pressure during the blasting of the Yellow River ice surface contact blasting and underwater blasting [5]. Zhang Mingfang summarized the relationship among technical parameters such as charge, ice breaking capacity, ice breaking hole spacing, ice discharge volume and other technical parameters based on the experimental data of ice blasting in Baotou area of the Yellow River

during the opening period [6]. Shin [7] established a three-dimensional finite element model of a solid ship and numerically simulated its dynamic response under explosive loads.

Previous studies have mostly focused on single blasting bombs, and there are few studies on double-layer blasting bombs. At present, the only publication on the blasting of a double-layered cartridge is Ye Xushuang. This study compares the double-layered charge with the uniform cross-section strip charge of the same size [8]. This thesis takes the Yellow River rapids monitoring and key technology research and demonstration projects for disaster prevention and mitigation as the subject. Through the theoretical analysis of ice breaking by underwater blasting, combined with the finite element software ANSYS/LS-DYNA, a three-dimensional model is established to study the effect of ice blasting under double-layer blasting charges, and to provide support for ice breaking research.

1.1 Underwater Explosive Load

Underwater-explosion ice breaking involves a variety of loads, which form a comprehensive dynamic process involving underwater shock waves, bubble pulsation, flow hysteresis, bubble collapse pulsating pressures, secondary cavitation loading, high-speed jets, and fluid–solid coupling effects [9]. For TNT explosives, the loads generated by underwater explosions are mainly shock waves. After the explosives detonate, the detonation products expand and compress the surrounding water to produce shock waves in the water. The shock waves propagate outward from the source of the explosion. The peak pressure of the bubble pulse

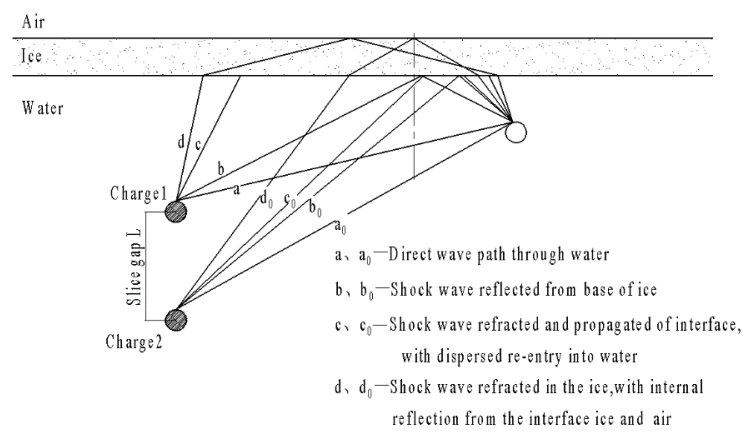


Fig. 1. Shock wave propagation process of underwater explosion with double charge

generated by the explosion does not exceed 20% of the shock wave pressure [10]. For a trinitrotoluene (TNT) charge, the main source of ice-breaking damage from underwater explosions is damage by shock waves. The propagation path of a group of shock waves under ice cover is shown in Fig. 2.

2. SIMULATION CALCULATION MODEL

2.1 Calculation Model Structure and Meshing

The nonlinear-dynamics finite-element software LS-DYNA was used to simulate the underwater ice blasting of a double-layer charge with a single-charge size of 3 kg, and five models with charge spacings of 50, 100, 150, 200, and 250 cm were constructed. The relationships between the ice-breaking damage diameter, the explosive layer spacing, the charge ratio, and the detonation time were studied. The simulation model was mainly composed of air, water, a TNT bag, and an ice layer. Due to the symmetry of the model, a 1/4-model was established. The overall model dimensions were 600 cm × 600 cm × 650 cm, the water body dimensions were 600 cm × 600 cm × 550 cm, the air domain dimensions were 600 cm × 600 cm × 100 cm, and the ice layer dimensions were 600 cm × 600 cm × 500 cm. and the medicine pack Obtained by adding *INITIAL_VOLUME_FRACTION_GEOMETRY.

The air, water, and TNT bag were defined by Eulerian grids, and the ice layer was defined by a Lagrangian grid. A non-reflective boundary condition was applied at the boundary of the axial surface of the air and water bodies. To prevent the sizes of the explosives from being too small and large differences of the grids causing large errors, the grids of the areas that needed to be filled with explosives were encrypted. The finite element model is shown in Fig. 2.

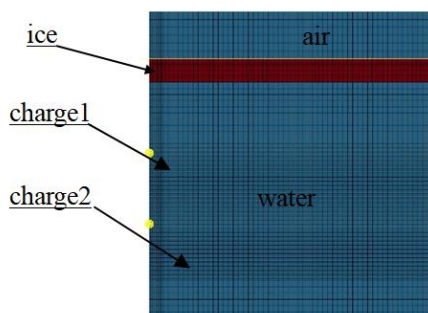


Fig. 2. Finite element model of numerical simulation

2.2 Material Model and Parameters

In the calculations, the material model of the formed TNT cartridge was the High-Explosive-Burn model, and the equation of state was the Jones–Wilkins–Lee (JWL) equation. The mechanical properties of ice are affected by the fragility of the hydrogen bonds between the molecules and the geometric characteristics of the crystal lattice [9]. Under pressure, ice exhibits an elastic, plastic, or brittle state, and its elastic and brittle mechanical properties increase as the temperature decreases, while plasticity becomes relatively weak. According to related data, the ultimate compressive strength of ice is 3.5–4.5 MPa at -5°C . The lower the temperature, the greater the tensile strength. The split tensile strength was determined by the concrete splitting tensile strength test method to be 0.82–1.18 MPa, and the ultimate tensile strength was 1.2–1.5 MPa. When the ice was broken by an explosion, the explosive load was quickly applied, and the ice body was mainly in the form of brittle failure. The ice body in this model was described by the ISOTROPIC_ELASTIC_FAILURE strength model. The tensile and compressive strengths were taken as damage standards. The tensile stress was 0.913 MPa, and the compressive stress was 9.15 MPa. The water material was represented by the NULL model, and the air and sediment were represented by the empty material model [11]. The specific material settings were as follows:

- 1) Main charge. The main charge was TNT, which was described by the high-energy combustion material model and the JWL equation of state. The main parameters were as follows: $\rho = 1.630 \text{ g/cm}^3$, $p\text{CJ} = 27.08 \text{ GPa}$, $D = 6930 \text{ m/s}$, $A = 371.2 \text{ GPa}$, $B = 32.1 \text{ GPa}$, $R1 = 4.15$, $R2 = 0.95$, and $\omega = 0.31$.
- 2) Water. The water medium was surrounded by a transmission and propagation boundary without reflection disturbances. The empty material water was described by the Grüneisen equation of state, and the density was $\rho = 0.99821 \text{ g/cm}^3$.
- 3) Air. The air was described by the empty material model and the EOS_LINEAR_POLYNOMIAL equation of state. The density was $\rho = 0.00125 \text{ g/cm}^3$.
- 4) Ice. The ice was described by the ELASTIC model. The density was $\rho = 0.897 \text{ g/cm}^3$, Young's modulus was $E = 0.0931 \text{ MPa}$, and Poisson's ratio was $PR = 0.33$.

3. NUMERICAL CALCULATION RESULTS AND ANALYSIS

3.1 Shock Wave Propagation and Pressure Change of Underwater Explosions with Double-layer Charge

After the explosive exploded in the water, the explosion products expanded sharply to produce a shock wave in the water. Fig. 3 shows the pressure cloud diagram of the ice layer and the water body when the distance between the cladding layers was 1.5 m. When $t = 30 \mu\text{s}$, the explosive detonation produced a shock wave in the water that spread. When $t = 70 \mu\text{s}$, the two layers of charge shock waves

began to converge and overlap. When $t = 86 \mu\text{s}$, the underwater-explosion shock wave generated by the upper charge continued to spread and began to affect the ice layer. At the lower edge of the ice layer, in the middle of the water body, the two-phase shock waves were superimposed to generate a new shock high-pressure zone. At the same time, the ice layer was rapidly subjected to tensile brittle failure under the action of the shock wave. The shock wave generated by the lower layer at $t = 218 \mu\text{s}$ continued to act on the ice layer, the emitted waves and sparse waves propagated and acted on the ice layer at the same time, and the damage to the ice cave was further aggravated.

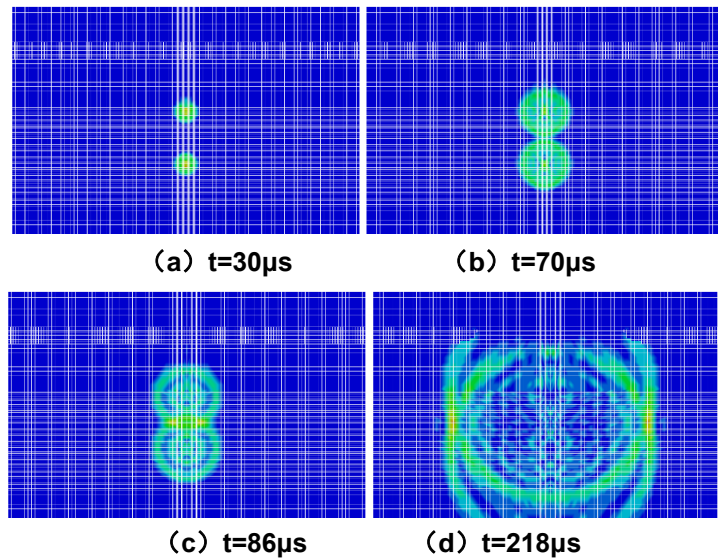


Fig. 3. Cloud chart of ice layer and water pressure at different time

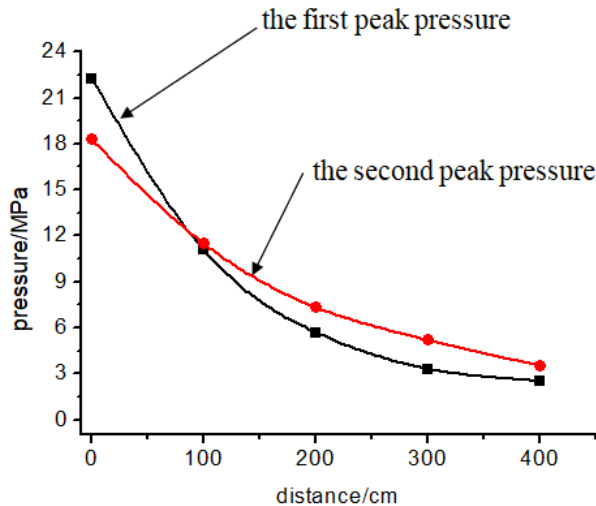


Fig. 4. Peak pressure of underwater explosion shock wave

Fig. 4 shows the peak pressure changes of the shock waves in the water at the lower edge of the ice sheet 0, 100, 200, 300, and 400 cm from the explosion source in the horizontal direction. At a position 0 cm directly above the explosion source, the maximum first peak pressure was 22.26 MPa. The peak pressures of the first and second wave peaks decreased with the increase in the distance from the explosion source, and this change conformed to the typical shock wave attenuation behavior. It is worth noting that the second peak pressure exceeded the first peak pressure at a position 100 cm from the explosion source, and the second peak pressure value was always greater than the first peak pressure. This was due to the shock wave at the air–water interface and the ice interface. Due to the superposition of the reflected shock wave and the positive-phase shock wave of the double-layer charge, along with the superposition phenomenon, the total peak pressure decayed slowly, and the shock wave pressure at the same distance was higher than of a single charge. For ice layers, such changes in underwater-explosion shock waves can further increase the damage and crack range of ice bodies.

3.2 Shock Wave Pressure in Water with Different Intervals between the Coatings

Using numerical simulation software, five charge spacings of 50, 100, 150, 200, and 250 cm were calculated, and the peak pressure values of the shock wave pressure in the water at the lower edge of the ice sheet were calculated at horizontal distances from the explosion source of

0, 100, 200, 300, and 400 cm. Fig. 5 shows the peak pressure values of the shock wave pressure at different distances from the explosion source. When the distance between the charge layers is the same, the farther the horizontal distance from the explosion source is, the smaller the shock wave peak value in the water at the lower edge of the ice sheet, and the smaller the distance between the charge layers, the higher the peak pressure of the shock wave. The distance between the charge layers mainly had a greater impact on the peak pressure value of the shock wave pressure within the range of 50–250 cm from the explosion source. The larger the distance, the greater the shock wave attenuation, and the impact of the coating interval was reduced. The spacing between the layers had almost no effect on the peak pressure value of the shock wave pressure up to spacings of 500 cm. The peak pressure values of the shock wave pressure in the water with spacings of 50–250 cm were more significantly affected by the wave superposition effect than those at spacings of less than 50 cm. The shock wave peak pressure was mainly generated by the upper charge. When the charge interval is 50, the peak value of the shock wave in the water under the ice layer directly above the explosion source is greater than the interval of other charge envelopes, due to the small charge interval, the shock wave has obvious superimposition.

According to the stress wave propagation behaviors described in Section 3.1, after the upper and lower charges detonated at the same time, stress waves were excited in the water, and the stress waves propagated around the

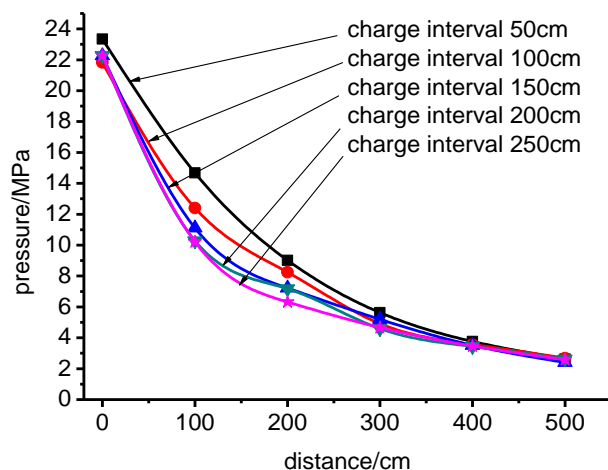
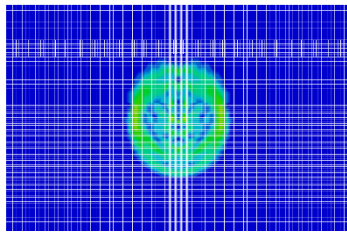
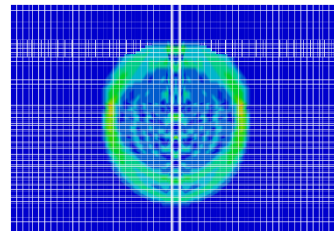


Fig. 5. Peak pressure of underwater explosion shock wave with different layer spacing

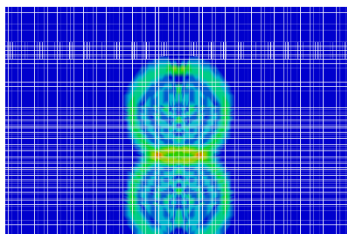


(a) The upper stress wave reaches the ice layer

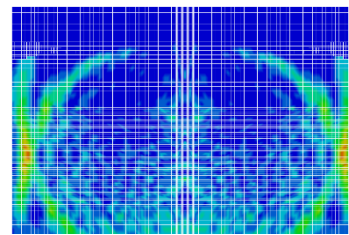


(b) The lower stress wave reaches the ice layer

Fig. 6. Cloud diagram of ice layer and water pressure change with a 0.5m interval between the coatings



(a) The upper stress wave reaches the ice layer



(b) The lower stress wave reaches the ice layer

Fig. 7. Cloud diagram of ice layer and water pressure change with a 2.5m interval between the coatings

center around the charges. Figs. 6 and 7 show the ice and water pressure cloud diagrams when the charge layer spacings were 0.5 and 2.5 m, respectively. Fig. 3 shows that after the upper and lower charge packs were detonated simultaneously, the lower charge pack was more excited than the upper charge pack. The stress wave acted on the ice layer after. The greater the distance between the two coatings, the greater the time interval between the two stress waves, and the weaker the superposition of the stress waves. To strengthen the superposition of the stress waves induced by the two charges, the time for the two stress waves to reach the ice layer should be controlled as much as possible. Therefore, it is necessary to further study the influence of the initiation time interval of the two charges on the shock wave pressure in the water layer.

3.3 Influence of Time Interval on Shock Wave Pressure in Water for Double-layer Charge Explosion

Various initiation time intervals of the two layers of the charge (Δt) were tested: 0, 10, 20, 30, 40, and 50 μs , and the changes of the peak pressure of the explosive shock wave when the charge

interval was 100 cm were determined, as shown in Fig. 8. Fig. 8 (a) shows the peak pressure change of the shock wave when the lower layer was delayed by Δt compared to the upper one. Fig. 8(b) shows the change of the peak pressure of the shock wave when the upper layer was delayed by Δt compared to the lower one. Fig. 8(a) shows that the time interval of the lower layer charge detonation delay had a small effect on the peak pressure of the shock wave in the water. The peak pressure of the shock wave was low. Regarding the upper and lower layers of the drug packet, no matter what the delay form, the smaller the distance from the center of the drug packet, the larger the shock wave peak value, and the shock wave superposition effect will not increase with the increase of the horizontal distance. The simulation results of the delay initiation of the upper charge in Table 1 showed that when the upper charge was delayed for 50 μs relative to the lower charge, the peak pressure of the shock wave directly above the source of the explosion was the largest, and then the delay time interval decreased. The peak pressure gradually decreased, and the degree of decrease became smaller and smaller. The results in Figs. 8(a) and 8(b) indicate that when the delay time of the upper charge was 30 μs ,

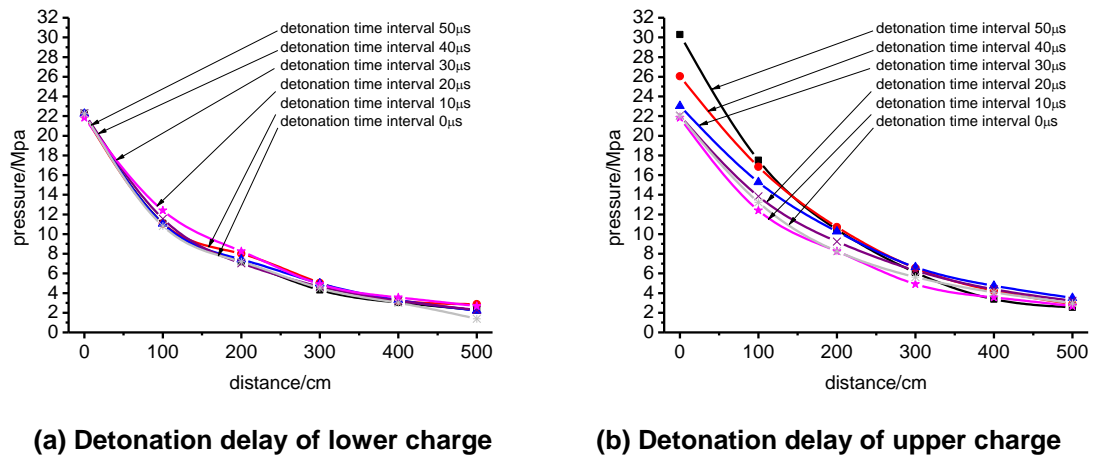


Fig. 8. Peak pressure of blast wave in water with different delay time

Table 1. Simulation results of delayed initiation of upper charge

Detonation interval / μ s	Coating spacing /cm	Distance from explosive source /cm	Shock wave peak pressure /MPa	Detonation interval / μ s	Coating spacing /cm	Distance from explosive source /cm	Shock wave peak pressure /MPa
0	100	0	21.82	30	100	0	23.03
	100	100	12.41		100	100	15.28
	100	200	8.25		100	200	10.26
	100	300	4.91		100	300	6.73
	100	400	3.56		100	400	4.74
	100	500	2.63		100	500	3.51
10	100	0	22.00	40	100	0	26.05
	100	100	13.23		100	100	16.84
	100	200	8.26		100	200	10.72
	100	300	5.62		100	300	6.54
	100	400	4.07		100	400	4.24
	100	500	2.98		100	500	2.88
20	100	0	22.04	50	100	0	30.3
	100	100	13.85		100	100	17.51
	100	200	9.24		100	200	10.47
	100	300	6.29		100	300	6.09
	100	400	4.38		100	400	3.83
	100	500	3.11		100	500	2.55

the shock wave peak pressure weakened relatively slowly, and when the horizontal distance from the explosion source was 500 cm, the shock wave still had the highest value compared to those under other conditions. Therefore, the upper layer of the charge detonated 30 μ s later than the lower layer of the charge, which could yield better shock wave energy utilization and obtain the best ice-breaking efficiency.

4. CONCLUSION

- (1) The peak pressure of the shock wave of a double-layer charge was determined.

Within a certain range, the second peak pressure of the lower charge was always greater than the first peak pressure of the upper charge. The attenuation of the second peak pressure was more sluggish, and this change was conducive to the enhancement of the damage to the ice and the growth of cracks.

- (2) The delay time of the initiation of the upper charge had little effect on the peak pressure of the shock wave in the water. The peak pressure of the shock wave in the water tended to be consistent, and the peak pressure of the shock wave directly above the explosion source was the largest.

(3) Compared with the delayed detonation of the lower layer of charge, the total peak pressure of the shock wave formed by the delay of the upper layer of the charge was larger at the same position. Numerical simulations showed that when the distance between the two layers of charge was 100 cm and the upper charge was detonated 30 μ s later than the lower charge, the shock wave energy utilization was improved, which was beneficial for the improvement of the ice breaking efficiency.

DISCLAIMER

The products used for this research are commonly and predominantly use products in our area of research and country. There is absolutely no conflict of interest between the authors and producers of the products because we do not intend to use these products as an avenue for any litigation but for the advancement of knowledge. Also, the research was not funded by the producing company rather it was funded by personal efforts of the authors.

FUNDING

This paper has received funding from the National Key Research and Development Program (2018YFC1508405)

COMPETING INTERESTS

Authors have declared that no competing interests exist.

REFERENCES

1. XIE Zhigang, ZENG He, LI Gen, et al. The Timing and method of eliminating the ice dam with airborne bomb by unmanned aerial vehicle [J]. Yellow River. 2021;43(2):70-73.
2. XIA Chang Fu. Research and practice of underwater ice jam breaking by manual operated blasting [J]. Blasting. 2014; 31(2):126-130.
3. MALCOLM M. Breaking ice with explosives [R]. USA: Cold Regions Research & Engineering Laboratory, US Army Corps of Engineers; 1982.
4. United States Army Corps of Engineers. Ice Engineering: Engineering and Design[M]. Department of the Army, US Army Corps of Engineers, Washington, DC 20314-1000;2002.
5. Liang Xiang Qian, Xiong Feng, Lu Xia Ling. Experimental research on underwater shock wave characteristic of ice blasting at yellow river [J]. Blasting. 2014;31(4):1-10.
6. Zhang Ming Fang, Zhang Fu Gui, Liang Xiang Qian, et al. Ice-breaking experimental study on blasting with concentrated charge [J]. Engineering Blasting. 2015;21(5):43-46.
7. Shin YS. Ship shock modeling and simulation for far field underwater explosion [J]. Computer and Structures. 2004;(82):2211-2219.
8. Ye Xu Shuang. Experimental study in double deck carge blasting [J]. Engineering Blasting. 1997;3(2):31-34.
9. Wang Ying, Xiao Wei, Yao Xiong Liangqin, et al. Fragmentation of ice cover subjected to underwater explosion shock wave load and its influence factors [J]. Explosion and Shock Waves. 2019;39(7):141-148.
10. Yu Jiang, Xiong Yan Fei, Wang Cong Yin, et al. Theoretical calculation of explosion damage range in ice medium and under ice layer [C]. Proceedings of the 7th National Conference on safety protection of engineering structures. Ningbo: Chinese Society of Mechanics, Chinese Society of Civil Engineering. 2009;7.9.
11. Huang Di. Study on the influence of underwater blasting vibration on surrounding buildings [D]. Hunan: Hunan University. 2019;39-42.

© 2021 Zhang et al.; This is an Open Access article distributed under the terms of the Creative Commons Attribution License (<http://creativecommons.org/licenses/by/4.0>), which permits unrestricted use, distribution, and reproduction in any medium, provided the original work is properly cited.

Peer-review history:

The peer review history for this paper can be accessed here:
<https://www.sdiarticle4.com/review-history/73619>